



Anti-hepatitis C virus RdRp activity and replication of novel anilinobenzothiazole derivatives

Huang-Kai Peng^a, Wei-Chun Chen^{b,c}, Ying-Ting Lin^c, Chin-Kai Tseng^{d,e}, Shiang-Yu Yang^f,
Cherng-Chyi Tzeng^g, Jin-Ching Lee^{c,h,*}, Shyh-Chyun Yang^{a,i,*}

^a School of Pharmacy, College of Pharmacy, Kaohsiung Medical University, Kaohsiung 807, Taiwan

^b Graduate Institute of Medicine, College of Medicine, Kaohsiung Medical University, Kaohsiung 807, Taiwan, ROC

^c Department of Biotechnology, College of Life Science, Kaohsiung Medical University, Kaohsiung 807, Taiwan, ROC

^d Institute of Basic Medical Sciences, College of Medicine, National Cheng Kung University, Tainan, Taiwan, ROC

^e Center of Infectious Disease and Signaling Research, College of Medicine, National Cheng Kung University, Tainan, Taiwan, ROC

^f Department of Dermatology, Kaohsiung Medical University Hospital, Kaohsiung 807, Taiwan, ROC

^g Department of Medicinal and Applied Chemistry, College of Life Science, Kaohsiung Medical University, Kaohsiung 807, Taiwan, ROC

^h Graduate Institute of Natural Products, College of Pharmacy, Kaohsiung Medical University, Kaohsiung 807, Taiwan, ROC

ⁱ Department of Fragrance and Cosmetic Science, College of Pharmacy, Kaohsiung Medical University, Kaohsiung 807, Taiwan, ROC

ARTICLE INFO

Article history:

Received 10 June 2013

Revised 29 July 2013

Accepted 5 August 2013

Available online 28 August 2013

Keywords:

Anilinobenzothiazole

Hepatitis C virus

RNA-dependent RNA polymerase

ABSTRACT

Hepatitis C virus (HCV) infection is a worldwide health problem. This can be attributed, in part, to the high mutation rate associated with RNA viral replication, which favors the emergence of drug resistance and limits the efficacy of current therapies. Here we report the continuation of our efforts to rationally design and synthesize a series of novel anilinobenzothiazole derivatives. We demonstrate that 2-(4-nitro-anilino)-6-methylenzothiazole (compound **14**) inhibited HCV RNA-dependent RNA polymerase (RdRp) activity and HCV RNA replication ($EC_{50} = 8 \pm 0.5 \mu\text{M}$) in a dose-dependent manner, consistent with a non-competitive model of inhibition (kinetic constant $K_i = 7.76 \mu\text{M}$). The best docking pose of compound **14** is located in the Thumb II Pocket, suggesting an inhibitory mechanism involving the docking of compound **14** that alters RdRp breathing. Combinations of compound **14** with interferon- α or other drugs potentially targeting HCV proteins, including telaprevir, PSI7977, or BMS790052, synergistically decreased the levels of HCV RNA.

© 2013 Elsevier B.V. All rights reserved.

1. Introduction

Hepatitis C virus (HCV) infection is a health problem in worldwide (Jahan et al., 2012). Only 50% of patients infected with HCV genotypes 1 and 4 experience a sustained virological response to current treatment with a combination of pegylated-interferon (IFN) and ribavirin (Hayashi and Takehara, 2006). Currently, two direct-acting antivirals, boceprevir and telaprevir, targeting HCV NS3 protease are approved by the U.S. Food and Drug Administration for the treatment of hepatitis C (Harrington et al., 2012; Soriano et al., 2013). This represents a significant beginning for drugs designed to inhibit specific viral proteins required for the virus life cycle, in contrast to the nonspecific antiviral activity of IFN. Current efforts to discover and develop DAAs have focused on those target-

ing the nonstructural protein NS5A and the RNA-dependent RNA polymerase (RdRp) NS5B (Chatel-Chaix et al., 2012). Therapies using combinations of DAAs or together with IFN are currently in clinical trials. However, side effects and low cure rates remain a problem. Furthermore, the high mutation rate associated with RNA viral replication favors the emergence of drug resistant strains and limits the efficacy of these therapies. Thus, the discovery of new drug targets or novel agents is urgently required to address these issues.

The pharmacophores of imidazole and cyclic benzimidazole have been designed from natural and semisynthetic products. These heterocyclic compounds show a wide spectrum of biological activities, including inhibition of the replication of pathogenic viruses such as human immunodeficiency virus (HIV) and HCV (Hari Babu et al., 2012). Furthermore, they inhibit the growth of cancer cells and mycobacteria and act as antioxidants and anti-inflammatory agents (Hari Babu et al., 2012). The anti-hepatitis B virus (HBV) activity of a 1-isopropylsulfonyl-2-amine benzimidazole derivative (I) (Li et al., 2007) and the inhibition of HCV NS5B by a benzimidazole-5-carboxylic acid derivative (II) (Ishida

* Corresponding authors. Address: Department of Biotechnology, College of Life Science, Kaohsiung Medical University, Kaohsiung 807, Taiwan, ROC. Tel.: +886 7 3121101x2369; fax: +886 7 3125339 (J.-C. Lee). Department of Fragrance and Cosmetic Science, College of Pharmacy, Kaohsiung Medical University, Kaohsiung 807, Taiwan, ROC. Tel.: +886 7 3121101x2662; fax: +886 7 3210683 (S.-C. Yang).

E-mail addresses: jclee@kmu.edu.tw (J.-C. Lee), scyang@kmu.edu.tw (S.-C. Yang).

et al., 2006) has been established. Moreover, the benzimidazole–coumarin conjugate derivatives (**III**) reported by Clercq et al. and the imidazopyridines (**IV**) also exhibit significant anti-HCV activity (Fig. 1) (Hwu et al., 2008; Vliegen et al., 2009).

Because the isosteric isomer approach has been applied extensively to drug design and based on the potent anti-HCV activity exhibited by our previously reported benzimidazole lead compound MSC015 (Lee et al., 2010), in the present study, we used molecular modeling to design new 2-anilinobenzothiazole derivatives (Fig. 2) that target the HCV RdRp and evaluated their abilities to inhibit HCV replication.

2. Material and methods

2.1. In vitro HCV RdRp activity assay

Renilla luciferase reporter activity developed as previous described represents the HCV RdRp activity (Lee et al., 2010). Huh7 cells were seeded in 24 wells plate at a density of 5×10^4 cells per well and transfected with p(+)FLuc(–)UTR-RLuc reporter plasmid (1 μ g). The transfected cells were treated with the compounds in various concentrations. After incubation at 37 °C for 4 days, cells lysates were harvested to measure the reporter gene expression inside cell by using the Dual-Glo™ Luciferase Assay System (Promega Corporation, Madison, WI) following the manufacturer's instructions. The relative activity of NS5B polymerase was determined by normalizing the level of *Renilla luciferase* against the level of Firefly luciferase.

2.2. Synthesis

The synthesized series of anilinobenzothiazole derivatives was prepared by our previously reported procedure (Peng et al., 2012). Reaction of the starting material, 2-chloro-6-methylbenzothiazole (**1**), with various anilines in the presence of EtOH produced **2–16** with overall yields of 63–95% (Supplementary Fig. S1). The preparation of anilinobenzothiazole derivatives is described in Supplementary information.

2.3. Cytotoxicity assay

Cell viability was determined by the colorimetric 3-(4,5-dimethylthiazol-2-yl)-5-(3-carboxymethoxyphenyl)-2-(4-sulfophenyl)-2H-

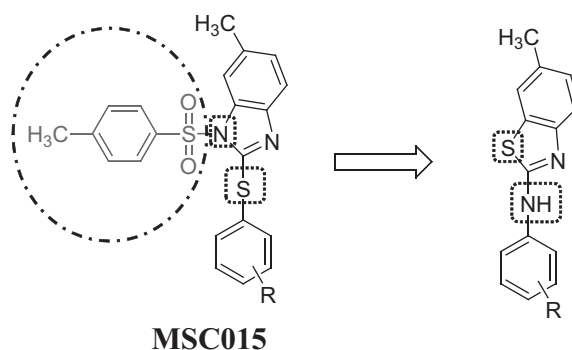


Fig. 2. Design concept using pharmacophores of MSC015 and anilinobenzothiazoles.

tetrazolium (MTS) assay. The Ava5 cells were seeded in 96-well plate at density of 5×10^3 cells per well and treated with the compounds at various concentrations. The CellTiter 96® Aqueous One Solution Cell Proliferation Assay (Promega, WI, USA) was used to determine the cell viability after 3 days incubation. The absorbance was detected at 490 nm.

2.4. Molecular modeling

All molecular modeling studies were performed on an Asus personal computer with Intel Core i7 2.67 GHz processor, running Windows 7 using ChemBioOffice 2010 (Kerwin, 2010) and Discovery Studio 2.1 (DS). (Discovery Studio 2.1, 2.1; Accelrys Software Inc.: San Diego, CA, USA, 2008). The receptor structure of HCV NS5B, cocrystallized with a synthetic inhibitor in the thumb domain, 4-bromo-2-[[[(3R,5S)-3,5-dimethylpiperidin-1-yl]carbonyl]aniline, was downloaded from the PDB data bank (<http://www.rcsb.org/pdb/index.html>; PDB code: 3CJ2) (Antonysamy et al., 2008). Compound structures were built with ChemBio3D of ChemBioOffice and minimized using the MMFF94 forcefield until a RMSD gradient of $0.05 \text{ kcal mol}^{-1} \text{ \AA}^{-1}$ was reached. The force field typing for partial charges was used CHARMm for inhibitors and proteins (Vanommeslaeghe et al., 2010, 2012; Vanommeslaeghe and MacKerell, 2012). Molecular docking were carried out using the DS LigandFit docking module. The 3CJ2 inhibitor present

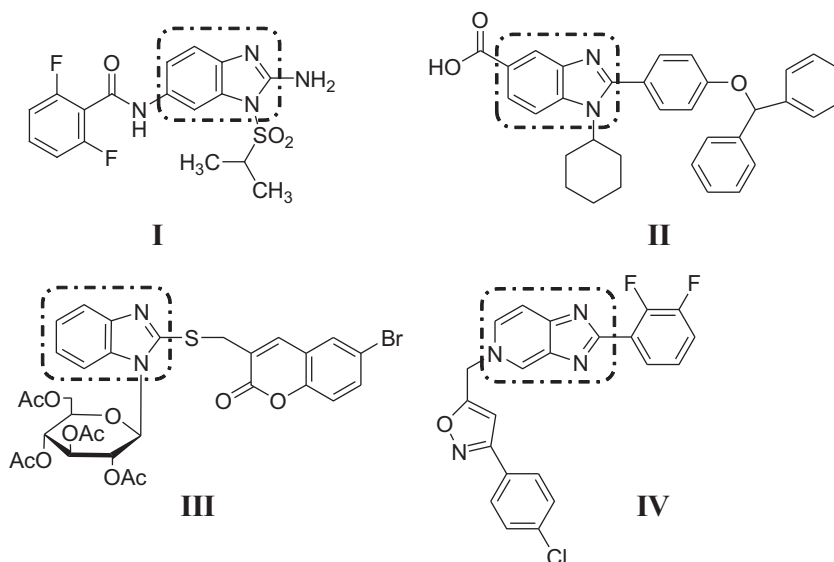


Fig. 1. Structures of HCV inhibitors.

in the thumb domain was used to define the binding site. The 3CJ2 inhibitor was manually removed from the active site before the docking experiment. PMF scoring function was used to measure the interaction energy between ligand pose and receptor (Muegge, 2006; Muegge and Martin, 1999). The output of LigandFit docking was visualized in the DS graphics environment, and the distances of hydrogen bonds were measured between the related non-hydrogen atoms of docking compounds and receptor residues.

2.5. K_i

A kinetic study of compounds against HCV RdRp using as in vitro coupled transcription and translation (TnT) reporter system was also achieved. The mode of inhibition and K_i value of the compound against RdRp is performed according to Lineweaver–Burk plot and Michaelis–Menten equation (Engel and Dalziel, 1969). The experiment were performed by using 100–1000 ng of (–)5'UTRΔC-RLuc RNA template with various concentrations of compound **14** (0–20 μ M) and a fixed concentration of methionine (33 μ M). Assay were carried out in the standard TnT reaction containing 500 ng of NS5BΔ21 protein. The luminescent readout was performed by Dual-Glo™ Luciferase Assay System (Promega). Following, the kinetic results, including K_i , K_m , competitive and non-competitive inhibition, were calculated according to the methods of Michaelis–Menten equation (Brandt et al., 1987).

2.6. In vitro HCV cellular replication assay

Huh7 cells harboring HCV Con1 genotype subgenomic replicon cells, designed Ava5, were kindly provided by Dr. C. Rice (Rockefeller University, New York, USA) and maintained in Dulbecco's modified Eagle's medium (DMEM) with 10% heat-inactivated fetal bovine serum, 5% Antibiotic–Antimycotic, 5% Non-essential amino acids, 1 mg/ml G418 and incubated at 37 °C with a 5% CO₂ supplement. The Ava5 cells were seeded in 24-wells plate at a density of 5×10^4 cells per well and treated with the compound at various concentrations. After incubation at 37 °C for 3 days, total cellular protein and RNA was extracted using RIPA and Trizol reagent (Invitrogen, Carlsbad, CA). The HCV protein synthesis and RNA replication were detected by Western blot and RT-qPCR, respectively, as previously described (Lee et al., 2011). The membranes were probed with monoclonal antibodies specific for HCV NS5B, (1:5000; Abcam, Cambridge, MA) or glyceraldehyde-3-phosphate dehydrogenase (GAPDH) (1:10,000; GeneTex, CA, USA). The signal was detected using an ECL detection kit (PerkinElmer, CT, USA). The levels of HCV subgenomic RNA were detected by RT-qPCR with primers corresponding to NS5B gene; forward primer: 5'-GGA AAC CAA GCT GCC CAT CA-3' and reverse primer: 5'-CCT CCA CGG ATA GAA GTT TA-3'. The copy number of HCV RNAs in each sample was normalized to cellular GAPDH (Forward primer: 5'-GTC TTC ACC ACC ATG GAG AA-3'; Reverse primer: 5'-ATG GCA TGG ACT GTG GTC AT-3') levels from three independent experiments with the ABI Step One Real-Time PCR-System (ABI Warrington, UK).

2.7. Analysis of drug synergism

Ava5 cells were treated with serially diluted compound **14** (1.25, 2.5, 5, 10, and 20 μ M) in combination with serially diluted IFN- α (7.5, 15, 30, and 60 U/ml), the HCV NS3/4A protease telaprevir (0.075, 0.15, 0.3, and 0.6 μ M), HCV NS5A inhibitor BMS790052 (1, 2, 4, and 8 pM) (Lemm et al., 2011), the RNA-dependent RNA polymerase nucleoside inhibitor PSI7977 (10, 20, 40, and 80 nM) (Lam et al., 2012). Combination index (CI) values were analyzed using the CalcuSyn software (Biosoft, Cambridge, UK) as previous described (Lee et al., 2011), a computer program based on the

method of Chou and Talalay (1984). The effect of multiple drug combinations is presented as antagonism (CI > 1), additivity (CI = 1), or synergism (CI < 1). In addition, traditional isobologram analysis was used to confirm the drug–drug interaction.

2.8. Statistical analysis

GraphPad Prism (Version 5.0, SmartDrawNet) was used for all statistical analysis and graphical illustrations. Data were presented as means \pm standards deviation for at least three independent experiments. The statistical significance was analyzed by using Student *t*-test. The significant difference was considered as $P < 0.05$ or $P < 0.01$.

3. Results and discussion

3.1. Assessment of the effects of anilinobenzothiazole derivatives on HCV replication and RdRp activity

The new anilinobenzothiazole derivatives, compounds **2–16**, were evaluated for their ability to inhibit HCV replication by treating cells harboring an HCV replicon designated Ava5. Total cellular RNA isolated from cells treated for 3 days was analyzed using a quantitative reverse transcriptase-polymerase chain reaction (qRT-PCR) assay. Cytotoxicity was simultaneously evaluated using the MTS assay. All the anilinobenzothiazole derivatives inhibited HCV RdRp activity to a similar extent (Table 1). Compounds **3**, **14**, and **15** exhibited more potent inhibition of HCV RNA replication (EC_{50} = 5, 8, and 10 μ M, respectively) compared with compounds **6**, **9**, **11**, and **13** (EC_{50} 25–60 μ M). These results indicate that the substitutions of anilinobenzothiazoles at the C2 and C4 positions conferred higher levels of activity. Moreover, the replacement of the electron-withdrawing group (EWG) on C4 imparted more potent activity, and the replacement of the electron-donating group (EDG) on C2 caused increased cytotoxicity. The substituent at the C4 position bearing EWG played a key role in inhibiting RdRp activity and viral replication. Not replacing EDG on the C2 position may produce a higher SI value. Therefore, these structure–activity relationships (SARs) indicate approaches for synthesizing more effective anilinobenzothiazoles.

To further evaluate the effects of compounds **2–16** on HCV RdRp activity, we used Huh7 cells transfected with the HCV RdRp-reporter plasmid p(+)/FLuc-(–)UTR-RLuc. Total cell lysates prepared from treated cells and controls were assayed for luciferase activity. As

Table 1
The anti-HCV RNA replication activity of anilinobenzothiazoles.

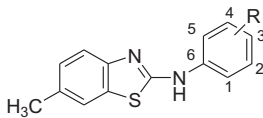
Compounds		EC_{50}	CC_{50}	SI
				
2	R = 4-CH ₃	>200	160	<1
3	R = 2,4-CH ₃	5	60	12
4	R = 3,5-CH ₃	>200	140	<1
5	R = 4-OCH ₃	>200	321	<2
6	R = 3,5-OCH ₃	28	28	1
7	R = 3,4,5-OCH ₃	50	200	4
8	R = 2-OCH ₂ Ph	>200	145	<1
9	R = 3-OCH ₂ Ph	50	50	1
10	R = 4-OCH ₂ Ph	80	141	1.8
11	R = 4-Cl	60	80	1.3
12	R = 4-Br, 2-Cl	>200	168	<1
13	R = 3-NO ₂	25	31	1.2
14	R = 4-NO ₂	8	303	37.8
15	R = 2-OH, 4-NO ₂	10	52	5.2
16	R = 2-OH, 4-COOH	>200	400	<2

Table 2
The anti-HCV RdRp activity of anilinobenzothiazoles.

Compounds	Inhibition % of RdRp		CC ₅₀
	5 μM	20 μM	
2	N.D.	N.D.	155
3	45	85	65
4	N.D.	N.D.	128
5	N.D.	N.D.	>200
6	N.D.	21	32
7	N.D.	N.D.	187
8	N.D.	N.D.	135
9	N.D.	35	53
10	N.D.	N.D.	130
11	14	31	81
12	N.D.	N.D.	180
13	12	38	40
14	32	76	>200
15	23	66	60
16	N.D.	N.D.	>200

N.D.: non-determined anti-RdRp activity.

shown in Table 2, compounds 6, 9, 11, and 13 (20 μM each) inhibited RdRp activity by 21–38%. In contrast, compounds 3, 14, and 15 inhibited activity by more than 66% (range, 66–85%). These results indicate that substitution at the C2' and C4' positions enhances inhibition of HCV RdRp activity by anilinobenzothiazoles.

The EC₅₀ for compound 14 (Fig. 3A) was the lowest, and after considering its cytotoxic effect, we further evaluated its effects on RdRp activity. Huh7 cells transfected with p(+)FLuc(–)UTR-RLuc and treated with compound 14 were assayed for luciferase activity and NS5B expression. Compound 14 inhibited RdRp activity in a concentration-dependent manner compared with untreated cells. The effective concentrations of compound 14 did not alter the level of NS5B expression (Fig. 3B). These results indicate that compound 14 is a potent inhibitor of HCV NS5B activity.

3.2. Kinetics of compound 14 inhibition of RdRp activity

To further characterize the effects of compound 14 on RdRp activity in vitro, we used a coupled transcription–translation

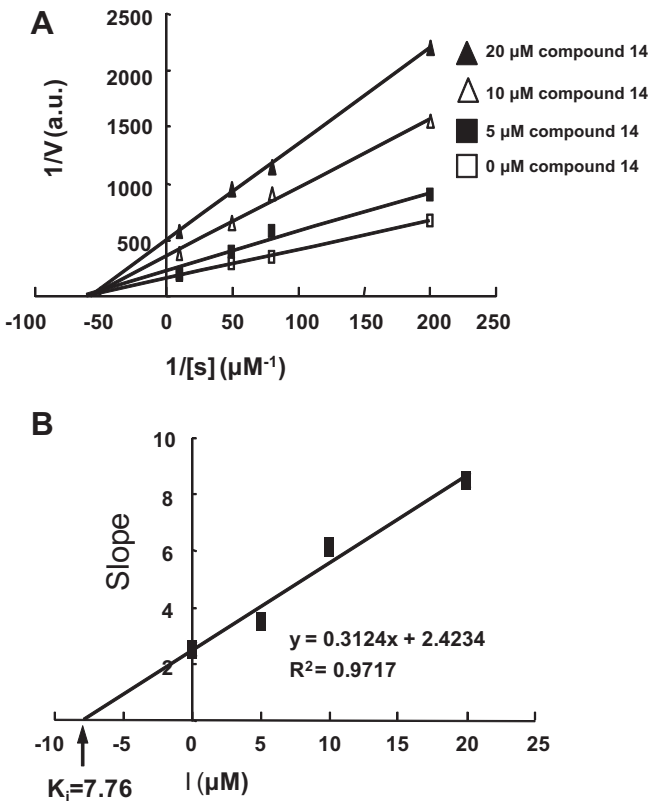


Fig. 4. Effect of compound 14 on HCV RdRp reaction kinetics. (A) The experiment was performed using the (–)5'UTRAC-RLuc RNA template, various concentrations of compound 14 (0–20 μM), and a constant concentration of methionine (33 μM). Assays were carried out using the standard TnT reaction mixture, which contained 500 ng of NS5BΔ21 as described in Section 2. HCV RdRp activity was determined by luminescence as described in Section 2. Each point represents the mean ± standard error of the mean of 3–5 determinations per point. (B) Lineweaver–Burk plot of the relationship between the dose (I/μM) and the inhibition rate (v) of compound 14 in the HCV RdRp assay. The straight line was fitted according to results of regression analysis using the Barber method.

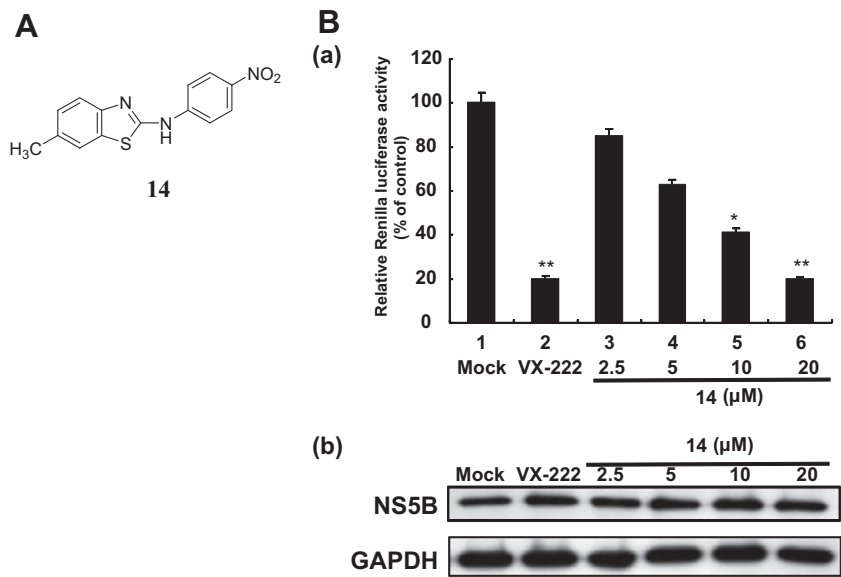


Fig. 3. Effect of compound 14 on HCV RdRp activity. (A) Structure of compound 14. (B) (a) Concentration-dependent reduction in HCV RdRp activity. For the RdRp activity assay, 1 μg of the RdRp reporter plasmid p(+)FLuc(–)UTR-RLuc and pcDNA3.1-NS5B were used to transiently cotransfect Huh7 cells. The medium used for transfection was replaced with complete medium containing various concentrations of compound 14 (0–20 μM) for 3 days. RLuc activity was normalized to that of FLuc, and VX-222 treatment served as the positive control. (b) Cell lysates were analyzed using western blotting with anti-HCV NS5B and anti-GAPDH (loading control) antibodies. Data represent the mean of normalized data ± standard deviation (SD), and the error bars denote SD for triplicate experiments. *P < 0.05; ** P < 0.01.

(TnT) system. In this assay, the RNA template is transcribed from the PCR product generated from (–)5'UTRΔC-RLuc encoding NS5B, the mRNA is translated in the presence of different concentrations of compound **14**, and the product is assayed for luciferase activity. The reaction kinetics shown in Fig. 4A indicated that compound **14** is a noncompetitive inhibitor, as is the positive control VX-222. Slopes (K_m/V_{max}) of the Lineweaver–Burk plots were then used to generate secondary plots to estimate K_i (Lineweaver and Burk, 1934). As shown in Fig. 4B, plots of compound **14** versus K_m/V_{max} show that $K_i = 7.76 \mu\text{M}$ with significant linearity ($r^2 = 0.9717$, $P < 0.005$). Taken together, these findings indicate that compound **14** specifically inhibits HCV RdRp activity. Because compound **14** significantly inhibited HCV RdRp activity in vivo and in vitro, we suggest that it is a potential hit compound against HCV replication for developing DAAs for treating chronic HCV infection.

3.3. Molecular docking analysis of compound **14** in the HCV RdRp

To enhance the rational design of anilinobenzothazole inhibitors, we performed molecular docking analysis of compound **14** to the crystal structure of HCV RdRp (Protein Data Bank code: 3CJ2). As shown in Fig. 5A, the best docking pose of compound **14** was located in the thumb domain of the enzyme, which is about 20–30 Å distant from the active site in the palm domain. Compound **14** displayed a similar binding mode compared with the inhibitor MSC015 that extends a moiety outward. We considered this structure unnecessary for our initial concept of design.

Compound **14** made the same contacts with surrounding residues as in the reference crystal ligand pose, SX3571 (Fig. 5B) (Antony et al., 2008). Four additional residues, Leu419, Leu497, Arg501, and Trp528 (light blue labels), make closer contacts with compound **14**. Trp528 makes an additional contact compared with SX3571, suggesting higher potency. Other surrounding residues shown are Met423, Ser476, Ile482, Ala486, Leu497, Asn527, and Ala529 (black labels). Therefore, we conclude that the compound **14** and MSC015 act through the same mechanism. Moreover, we also docked the standard compound VX-222, for which X-ray crystallography data have not been reported, to the same Thumb II Pocket of HCV RdRp. As shown in Fig. 5C, the best docking pose indicates that VX-222 makes close contacts with Leu419, Met423, Ser476, Tyr477, Ile482, Leu497, Arg501, Trp528, and Ala529. Moreover, this putative docking pose makes close contacts with Leu419, Met423, and Ile482, which is consistent with a previous study of an RdRp mutant that was not inhibited by VX-222 (Le Pogam et al., 2006).

3.4. Effect of compound **14** on cells harboring an HCV replicon

To assess the effects of compound **14** on HCV replication, Ava5 cells were incubated with compound **14** (0–20 μM) for 3 days and then analyzed using western blotting and qRT-PCR. Compound **14** significantly inhibited HCV protein expression compared with the control (Fig. 6A). Moreover, it inhibited HCV RNA synthesis (EC_{50} value of $8 \pm 0.5 \mu\text{M}$); however, significant cytotoxicity was not detected at the effective concentrations (Fig. 6B). These data are consistent with the effects of compound **14** on the JFH-1 system that produces infectious virus. Thus, there were significant reductions in the HCV RNA levels (Fig. 6C).

3.5. Effects of compound **14** on HCV replication in combination with either IFN- α or viral enzyme inhibitors

Combination therapy of HCV infection using drugs with different modes of action may improve efficacy and reduce side effects of treatment with IFN alone. Moreover, treatments that do not rely

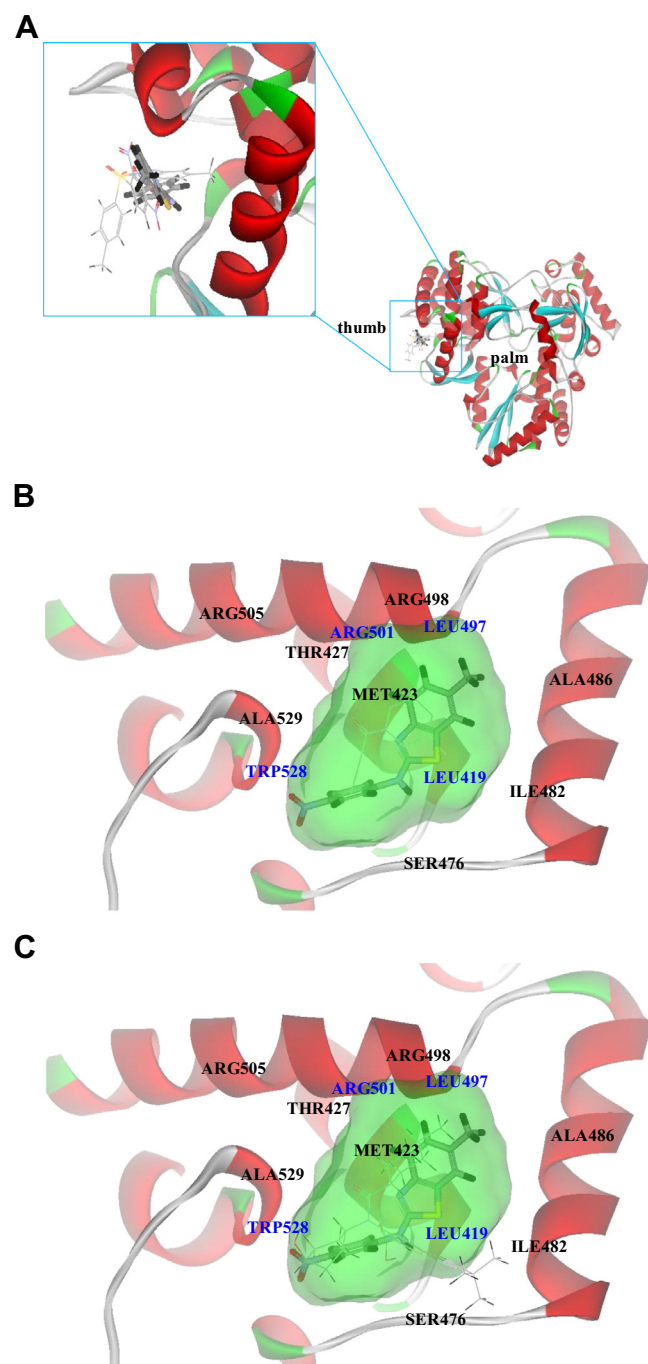


Fig. 5. Mechanism of binding of compound **14**, an allosteric inhibitor of HCV RdRp. (A) The best docking pose of compound **14** (stick figures) is located in the thumb domain of HCV RdRp, while MSC015 (lines) extends a fragment outward, which we consider unnecessary. Note that this binding site differs from the nucleoside class of drugs (palm domain) in that the structural effect differs. Inhibition of HCV RdRp breathing may explain the inhibitory mechanism. (B) The residues surrounding the binding pocket of compound **14** (stick) and SX3571 (line). (C) The surrounding residues of the binding pocket of compound **14** (stick) and VX-222 (line).

on interferon will represent a significant breakthrough. Therefore, we treated Ava5 cells with compound **14** and either IFN- α , telaprevir (an NS3/4A protease inhibitor approved by the United States Food and Drug Administration in May 2011), PSI7977 (an NS5B inhibitor) (Jesudian et al., 2012; Lam et al., 2012), or BMS790052 (an NS5A complex inhibitor) (Lemm et al., 2011) at different concentrations in constant ratios for 3 days. The effects on viral RNA synthesis were evaluated using qRT-PCR. Each of the combinations

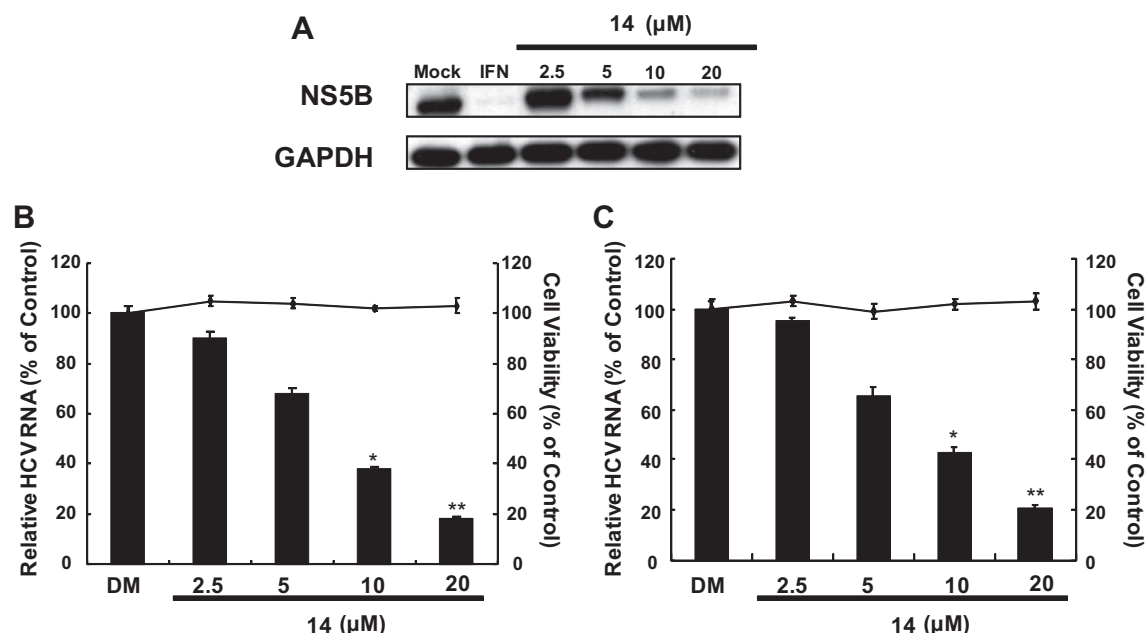


Fig. 6. Effect of compound **14** on HCV protein expression and RNA replication. (A) Compound **14** inhibited HCV protein synthesis in a concentration-dependent manner. Ava5 cells were incubated with various concentrations of compound **14** (2.5, 5, 10, and 20 μ M) for 3 days. IFN- α treatment served as the positive control. Cell lysates were analyzed using western blotting with anti-HCV NS5B and anti-GAPDH (loading control) antibodies. Compound **14** inhibited HCV RNA replication in the (B) HCV replicon and (C) HCV JFH-1 infectious systems. Ava5 cells or JFH-1-infected Huh-7 cells were treated with various concentrations of compound **14** (2.5, 5, 10, and 20 μ M) for 3 days. Total cellular RNA was extracted to quantify the relative HCV RNA levels normalized to the levels of *Gapdh* mRNA expression using qRT-PCR. Relative cell viability was measured using the MTS assay. Data are shown as the mean of the normalized data \pm SD. Error bars denote SD for triplicate experiments. * P < 0.05; ** P < 0.01.

Table 3
Effects of compound **14** in combination with different inhibitors of HCV replication

Combination compound	CI values at			Influence
	ED ₅₀	ED ₇₅	ED ₉₀	
IFN- α	0.7	0.6	0.5	Synergistic
Telaprevir	0.7	0.5	0.4	Synergistic
PSI7977	0.9	0.8	0.7	Synergistic
BMS790052	0.5	0.4	0.3	Synergistic

Various concentrations of compound **14** and HCV inhibitors, IFN- α , telaprevir, PSI7977, or BMS-790052 were used to treat Ava5 cells for 3 days. Inhibition of HCV replication, as indicated by HCV RNA levels, was determined using qRT-PCR. The CI value for an effective dose of 50% (ED₅₀), 75% (ED₇₅), or 90% (ED₉₀) was calculated using CalcuSyn software. The degree of interaction of the potential drugs was evaluated according to the CI value as follows: values of <1, 1, and >1 indicate synergistic, additive, and antagonistic effects, respectively.

synergistically reduced HCV RNA levels compared with controls. The combination index (CI) for values <1 for ED₅₀, ED₇₅, and ED₉₀ (range, 0.3–0.9) is shown in Table 3. These results suggest that compound **14** is a promising adjuvant for treating patients with chronic HCV infection.

In conclusion, we rationally designed and synthesized a series of novel anilinothiazole derivatives and evaluated their effects on HCV RdRp and replication of the viral genome. We here demonstrated that compound **14** (20 μ M) inhibited HCV RdRp activity by 76%. Inhibition was noncompetitive and dose-dependent. The EC₅₀ value was 8 ± 0.5 μ M in Ava5 cells and HCV JFH-1 systems. Analysis of SAR revealed that the substituents on the C4' position were crucial for inhibitory activity. Molecular docking analysis revealed that the best binding pose of compound **14** is located in the Thumb II Pocket of HCV RdRp. Compound **14** also acted synergistically with IFN- α , telaprevir, PSI7977, or BMS790052 in reducing HCV RNA levels. These results indicate that compound **14** shows promise as a potential hit compound for further development of anti-HCV drugs.

Acknowledgments

We thank the National Science Council of the Republic of China, the National Science Council of Taiwan (grant numbers NSC101-2113-M-037-008-MY3 and NSC100-2311-B-037-001), and the Kaohsiung Medical University Research Foundation, Taiwan (KMUR014) for financial support. We thank the National Center for High-Performance Computing for providing computer resources and chemical database services. We are grateful to Dr. Charles Rice (Rockefeller University and Aapth, LCC, USA) for kindly supporting the Con1b replicon plasmid, human hepatoma cells (Huh-7), and the HCV subgenomic replicon-containing cell line (Ava5) as well as Dr. T. Wakita (National Institute of Infectious Diseases, Japan) for providing the JFH-1 plasmid.

Appendix A. Supplementary data

Supplementary data associated with this article can be found, in the online version, at <http://dx.doi.org/10.1016/j.antiviral.2013.08.009>.

References

- Antonyamy, S.S., Aubol, B., Blaney, J., Browner, M.F., Giannetti, A.M., Harris, S.F., Hebert, N., Hendle, J., Hopkins, S., Jefferson, E., Kissinger, C., Leveque, V., Marciano, D., McGee, E., Najera, I., Nolan, B., Tomimoto, M., Torres, E., Wright, T., 2008. Fragment-based discovery of hepatitis C virus NS5b RNA polymerase inhibitors. *Bioorg. Med. Chem. Lett.* 18, 2990–2995.
- Brandt, R.B., Laux, J.E., Yates, S.W., 1987. Calculation of inhibitor K_i and inhibitor type from the concentration of inhibitor for 50% inhibition for Michaelis–Menten enzymes. *Biochem. Med. Metab. Biol.* 37, 344–349.
- Chatel-Chaix, L., Germain, M.A., Gotte, M., Lamarre, D., 2012. Direct-acting and host-targeting HCV inhibitors: current and future directions. *Curr. Opin. Virol.* 2, 588–598.
- Chou, T.C., Talalay, P., 1984. Quantitative analysis of dose–effect relationships: the combined effects of multiple drugs or enzyme inhibitors. *Adv. Enzyme Regul.* 22, 27–55.

- Engel, P.C., Dalziel, K., 1969. Kinetic studies of glutamate dehydrogenase with glutamate and norvaline as substrates. Coenzyme activation and negative homotropic interactions in allosteric enzymes. *Biochem. J.* 115, 621–631.
- Hari Babu, L., Perumal, S., Balasubramanian, M.P., 2012. Myrtenal attenuates diethylnitrosamine-induced hepatocellular carcinoma in rats by stabilizing intrinsic antioxidants and modulating apoptotic and anti-apoptotic cascades. *Cell Oncol. (Dordr)* 35, 269–283.
- Harrington, P.R., Zeng, W., Naeger, L.K., 2012. Clinical relevance of detectable but not quantifiable hepatitis C virus RNA during boceprevir or telaprevir treatment. *Hepatology* 55, 1048–1057.
- Hayashi, N., Takehara, T., 2006. Antiviral therapy for chronic hepatitis C: past, present, and future. *J. Gastroenterol.* 41, 17–27.
- Hwu, J.R., Singha, R., Hong, S.C., Chang, Y.H., Das, A.R., Vliegen, I., De Clercq, E., Neyts, J., 2008. Synthesis of new benzimidazole–coumarin conjugates as anti-hepatitis C virus agents. *Antiviral Res.* 77, 157–162.
- Ishida, T., Suzuki, T., Hirashima, S., Mizutani, K., Yoshida, A., Ando, I., Ikeda, S., Adachi, T., Hashimoto, H., 2006. Benzimidazole inhibitors of hepatitis C virus NS5B polymerase: identification of 2-[(4-diarylmethoxy)phenyl]-benzimidazole. *Bioorg. Med. Chem. Lett.* 16, 1859–1863.
- Jahan, S., Ashfaq, U.A., Qasim, M., Khaliq, S., Saleem, M.J., Afzal, N., 2012. Hepatitis C virus to hepatocellular carcinoma. *Infect. Agents Cancer* 7, 2.
- Jesudian, A.B., Gambarin-Gelwan, M., Jacobson, I.M., 2012. Advances in the treatment of hepatitis C virus infection. *Gastroenterol. Hepatol. (N. Y.)* 8, 91–101.
- Kerwin, S.M., 2010. ChemBioOffice Ultra 2010 suite. *J. Am. Chem. Soc.* 132, 2466–2467.
- Lam, A.M., Espiritu, C., Bansal, S., Micolochick Steuer, H.M., Niu, C., Zennou, V., Keilman, M., Zhu, Y., Lan, S., Otto, M.J., Furman, P.A., 2012. Genotype and subtype profiling of PSI-7977 as a nucleotide inhibitor of hepatitis C virus. *Antimicrob. Agents Chemother.* 56, 3359–3368.
- Le Pogam, S., Kang, H., Harris, S.F., Leveque, V., Giannetti, A.M., Ali, S., Jiang, W.R., Rajyaguru, S., Tavares, G., Oshiro, C., Hendricks, T., Klumpp, K., Symons, J., Browner, M.F., Cammack, N., Najera, I., 2006. Selection and characterization of replicon variants dually resistant to thumb- and palm-binding nonnucleoside polymerase inhibitors of the hepatitis C virus. *J. Virol.* 80, 6146–6154.
- Lee, J.C., Chen, W.C., Wu, S.F., Tseng, C.K., Chiou, C.Y., Chang, F.R., Hsu, S.H., Wu, Y.C., 2011. Anti-hepatitis C virus activity of *Acacia confusa* extract via suppressing cyclooxygenase-2. *Antiviral Res.* 89, 35–42.
- Lee, J.C., Tseng, C.K., Chen, K.J., Huang, K.J., Lin, C.K., Lin, Y.T., 2010. A cell-based reporter assay for inhibitor screening of hepatitis C virus RNA-dependent RNA polymerase. *Anal. Biochem.* 403, 52–62.
- Lemm, J.A., Leet, J.E., O'Boyle 2nd, D.R., Romine, J.L., Huang, X.S., Schroeder, D.R., Alberts, J., Cantone, J.L., Sun, J.H., Nower, P.T., Martin, S.W., Serrano-Wu, M.H., Meanwell, N.A., Snyder, L.B., Gao, M., 2011. Discovery of potent hepatitis C virus NS5A inhibitors with dimeric structures. *Antimicrob. Agents Chemother.* 55, 3795–3802.
- Li, Y.F., Wang, G.F., Luo, Y., Huang, W.G., Tang, W., Feng, C.L., Shi, L.P., Ren, Y.D., Zuo, J.P., Lu, W., 2007. Identification of 1-isopropylsulfonyl-2-amine benzimidazoles as a new class of inhibitors of hepatitis B virus. *Eur. J. Med. Chem.* 42, 1358–1364.
- Lineweaver, H., Burk, D., 1934. The determination of enzyme dissociation constants. *J. Am. Chem. Soc.* 56, 658–666.
- Muegge, I., 2006. PMF scoring revisited. *J. Med. Chem.* 49, 5895–5902.
- Muegge, I., Martin, Y.C., 1999. A general and fast scoring function for protein–ligand interactions: a simplified potential approach. *J. Med. Chem.* 42, 791–804.
- Peng, H.K., Lin, C.K., Yang, S.Y., Tseng, C.K., Tzeng, C.C., Lee, J.C., Yang, S.C., 2012. Synthesis and anti-HCV activity evaluation of anilinoquinoline derivatives. *Bioorg. Med. Chem. Lett.* 22, 1107–1110.
- Soriano, V., Labarga, P., Fernandez-Montero, J.V., Benito, J.M., Poveda, E., Rallon, N., Sanchez, C., Vispo, E., Barreiro, P., 2013. The changing face of hepatitis C in the new era of direct-acting antivirals. *Antiviral Res.* 97, 36–40.
- Vanommeslaeghe, K., Hatcher, E., Acharya, C., Kundu, S., Zhong, S., Shim, J., Darian, E., Guvench, O., Lopes, P., Vorobyov, I., Mackerell Jr., A.D., 2010. CHARMM general force field: a force field for drug-like molecules compatible with the CHARMM all-atom additive biological force fields. *J. Comput. Chem.* 31, 671–690.
- Vanommeslaeghe, K., MacKerell Jr., A.D., 2012. Automation of the CHARMM General Force Field (CGenFF) I: bond perception and atom typing. *J. Chem. Inf. Model.* 52, 3144–3154.
- Vanommeslaeghe, K., Raman, E.P., MacKerell Jr., A.D., 2012. Automation of the CHARMM General Force Field (CGenFF) II: assignment of bonded parameters and partial atomic charges. *J. Chem. Inf. Model.* 52, 3155–3168.
- Vliegen, I., Paeshuyse, J., De Burghgraeve, T., Lehman, L.S., Paulson, M., Shih, I.H., Mabery, E., Boddeker, N., De Clercq, E., Reiser, H., Oare, D., Lee, W.A., Zhong, W., Bondy, S., Purstinger, G., Neyts, J., 2009. Substituted imidazopyridines as potent inhibitors of HCV replication. *J. Hepatol.* 50, 999–1009.